

CHAPTER 5

LATERAL LOADING OF A SHAFT IN LAYERED SOIL USING THE STRAIN WEDGE MODEL

5.1 INTRODUCTION

The strain wedge (SW) model is an approach that has been developed to predict the response of a flexible pile under lateral loading (Norris 1986, Ashour et al. 1996 and Ashour et al. 1998). The main concept associated with the SW model is that traditional one-dimensional Beam on Elastic Foundation (BEF) pile response parameters can be characterized in terms of three-dimensional soil-pile interaction behavior. The SW model was initially established to analyze a free-head pile embedded in one type of uniform soil (sand or clay). However, the SW model has been improved and modified through additional research to accommodate a laterally loaded pile embedded in multiple soil layers (sand and clay). The SW model has been further modified to include the effect of pile head conditions on soil-pile behavior. The main objective behind the development of the SW model is to solve the BEF problem of a laterally loaded pile based on the envisioned soil-pile interaction and its dependence on both soil and pile properties.

The problem of a laterally loaded pile in layered soil has been solved by Reese (1977) as a BEF based on modeling the soil response by p-y curves. However, as mentioned by Reese (1983), the nonlinear p-y curve employed does not account for soil continuity and pile properties such as pile stiffness, pile cross-section shape and pile head conditions.

The SW model was initially developed to assess the response of a laterally loaded long (slender) pile (diameter < 3 ft). As a result, the effect of the vertical side shear (V_v) along the side of a large diameter shaft should be integrated in the SW model analysis to account for such a significant parameter in the analysis of large diameter shafts (Fig. 5-1). In addition, the characterization of the intermediate and short shafts should be incorporated in the SW model analysis to cover broader aspects of the shaft/pile analysis.

5.2 THE THEORETICAL BASIS OF STRAIN WEDGE MODEL CHARACTERIZATION

The SW model parameters are related to an envisioned three-dimensional passive wedge of soil developing in front of the pile. The basic purpose of the SW model is to relate stress-strain-strength behavior of the soil in the wedge to one-dimensional BEF parameters. The SW model is, therefore, able to provide a theoretical link between the more complex three-dimensional soil-pile interaction and the simpler one-dimensional BEF characterization. The previously noted correlation between the SW model response and BEF characterization reflects the following interdependence:

- the horizontal soil strain (ϵ) in the developing passive wedge in front of the pile to the deflection pattern (y versus depth, x) of the pile;
- the horizontal soil stress change ($\Delta\sigma_h$) in the developing passive wedge to the soil-pile reaction (p) associated with BEF behavior; and
- the nonlinear variation in the Young's modulus ($E = \Delta\sigma_h/\epsilon$) of the soil to the nonlinear variation in the modulus of soil subgrade reaction ($E_s = p/y$) associated with BEF characterization.

The analytical relations presented above reflect soil-pile interaction response characterized by the SW model that will be illustrated later. The reason for linking the SW model to BEF analysis is to allow the appropriate selection of BEF parameters to solve the following fourth-order ordinary differential equation to proceed.

$$EI \left(\frac{d^4 y}{d^4 x} \right) + E_s(x) y + P_x \left(\frac{d^2 y}{d^2 x} \right) + \left(\frac{d^2 M_R}{d^2 x} \right) = 0 \quad (5-1)$$

where M_R is the resisting bending moment per unit length induced along the shaft length (x) due to the vertical side shear (V_V) (Fig. 5-1). The closed form solution of the basic form of the above equation has been obtained by Matlock and Reese (1961) for the case of uniform soil. In order to appreciate the SW model's enhancement of BEF analysis, one should first consider the governing analytical formulations related to the passive wedge in front of the shaft, the soil's

stress-strain and the vertical side shear (t-z curve) formulations, and the related soil-pile interaction.

5.3 SOIL PASSIVE WEDGE CONFIGURATION

The SW model represents the mobilized passive wedge in front of the pile which is characterized by base angles, ϕ_m and β_m , the current passive wedge depth h , and the spread of the wedge fan angle, ϕ_m (the mobilized friction angle of soil). The horizontal stress change at the passive wedge face, $\Delta\sigma_h$, and side shear, τ , act as shown in Fig. 5-2. One of the main assumptions associated with the SW model is that the deflection pattern of the pile is taken to be linear over the controlling depth of the soil near the pile top resulting in a linearized deflection angle, δ , as seen in Fig. 5-3.

The SW model makes the analysis simpler because forces (F_1) on the opposite faces cancel, but the real zone of stress is like the dashed outline shown in Fig. 5-4b which includes side shear influence ($\hat{\delta}$) on the shape of the strained zone. However, the $\hat{\delta}$ perpendicular to the face of the pile is still considered in the SW model analysis. As seen in Fig. 5-4c, the horizontal equilibrium in the SW wedge model is based on the concepts of the conventional triaxial test. The soil at the face of the passive wedge is represented by a soil sample in the conventional triaxial test where $\bar{\sigma}_{vo}$ (i.e. $K = 1$) and the horizontal stress change, $\Delta\sigma_h$, (from pile loading) are the confining and deviatoric stresses in the triaxial test, respectively.

The relationship between the actual (closed form solution) and linearized deflection patterns of long pile/shaft has been established by Norris (1986) ($h/X_o = 0.69$). As seen in 5-5, the relationship (h/X_o) between the actual and linearized deflection for the short shaft is equal to 1, and varies for the intermediate shafts from 0.69 at ($L/T = 4$) to 1 at ($L/T = 2$). As presented in Chapter 2, L is the embedded length of the shaft and T is the initial relative shaft stiffness.

It should be noted that the idea of the change in the full passive wedge (mobilized passive wedge at different levels of deflection) employed in the SW model has been shown experimentally by Hughes and Goldsmith (1978) and previously established by Rowe (1956).

Changes in the shape and depth of the upper passive wedge, along with changes in the state of loading and shaft/pile deflection, occur with change in the uniform strain (ϵ) in the developing passive wedge. As seen in Fig. 5-6, two mobilized (tip to tip) passive wedges are developed in soil in front of the short shaft. Because of the shaft straight-line deflection pattern with a deflection angle δ , the uniform soil strain (ϵ) will be the same in both (i.e. upper and lower) passive wedges.

As shown in Figs. 5-5 and 5-6, the deflection pattern is no longer a straight line for the intermediate shaft, and the lower passive wedge has a curved shape that is similar to the deflection pattern. Accordingly, the soil strain (ϵ_x) at depth x below the zero crossing will not be uniform and will be evaluated in an iterative method based on the associated deflection at that depth (Fig. 5-6c)

The lateral response of the short shaft is governed by both (upper and lower) developed passive wedges (Fig. 5-6). However, with the intermediate shaft, less soil strain (i.e. stress on soil) develops in the lower passive soil wedge (the inverted wedge below the point of zero crossing) compared to the upper one (Fig. 5-6). The non-uniform soil strain (ϵ_x) in the lower passive soil wedge (Fig. 5-6c) becomes much smaller compared to the strain in the upper soil wedge when the shaft deflection approaches the deflection pattern of the long shaft. Since the lateral deflection of the long pile/shaft below the zero crossing is always very small, the associated soil strain and developing passive wedge will be very small as well. Consequently, the developing upper passive soil wedge (and uniform strain therein) dominates the lateral response of the long pile/shaft; hence the adopted name “strain wedge” (SW).

As seen in Figs. 5-3 and 5-6, the configuration of the wedge at any instant of load and, therefore, base angle

$$\Theta_m = 45 - \frac{j_m}{2} \quad (5-2)$$

mobilized friction angle, ϕ_m , and wedge depth, h , is given by the following equation:
or its complement

$$\mathbf{b}_m = 45 + \frac{\mathbf{j}_m}{2} \quad (5-3)$$

The width, \overline{BC} , of the wedge face at any depth is

$$\overline{BC} = D + (h - x) 2 \tan \mathbf{b}_m \tan \mathbf{j}_m \quad (5-4)$$

where x denotes the depth below the top of the studied passive wedge, and D symbolizes the width of the pile cross-section. It should be noted that the SW model is based upon an effective stress analysis of both sand and clay soils. As a result, the mobilized fanning angle, ϕ_m , is not zero in clay soil as assumed by Reese (1958, 1983).

The above equations are applied to the upper and lower passive wedges in the case of short and intermediate shafts where x for any point on the lower passive wedge (Fig. 5-6c) is measured downward from the zero crossing and replaces the term $(h - x)$ in Eqn. 5-4. Therefore,

$$\mathbf{e}_x = \mathbf{e} (y_x / x) / \mathbf{d} = \mathbf{e} \left(\frac{\mathbf{d}_x}{\mathbf{d}} \right) \quad (5-5)$$

where ε and δ are the uniform soil strain and linearized shaft deflection angle of the upper passive wedge, respectively. y_x and δ_x are the shaft deflection and secant deflection angle at depth x below the zero crossing (Fig. 5-6c).

5.4 STRAIN WEDGE MODEL IN LAYERED SOIL

The SW model can handle the problem of multiple soil layers of different types. The approach employed, which is called the multi-sublayer technique, is based upon dividing the soil profile and the loaded pile into sublayers and segments of constant thickness, respectively, as shown in Fig. 5-7. Each sublayer of soil is considered to behave as a uniform soil and have its own properties according to the sublayer location and soil type. In addition, the multi-sublayer technique depends on the deflection pattern of the embedded pile being continuous regardless of the variation of soil types. However, the depth, h , of the deflected portion of the pile is controlled by the stability analysis of the pile under the conditions of soil-pile interaction. The effects of the soil and pile properties are associated with the soil reaction along the pile by the

Young's modulus of the soil, the stress level in the soil, the pile deflection, and the modulus of subgrade reaction between the pile segment and each soil sublayer. To account for the interaction between the soil and the pile, the deflected part of the pile is considered to respond as a continuous beam loaded with different short segments of uniform load and supported by nonlinear elastic supports along soil sublayers, as shown in Fig. 5-8. At the same time, the point of zero deflection (X_0 in Fig. 5-5) for a pile in a particular layered soil varies according to the applied load and the soil strain level.

The SW model in layered soil provides a means for distinguishing layers of different soil types as well as sublayers within each layer where conditions (ϵ_{50} , SL, ϕ_m) vary even though the soil and its properties ($\bar{\gamma}$, e or D_r , ϕ , etc.) remain the same. As shown in Fig. 5-9, there may be different soil layers and a transition in wedge shape from one layer to the next, with all components of the compound wedge having in common the same depth h . In fact, there may be a continuous change over a given sublayer; but the values of stress level (SL) and mobilized friction angle (ϕ_m) at the middle of each sublayer of height, H_i , are treated as the values for the entire sublayer.

As shown in Fig. 5-9, the geometry of the compound passive wedge depends on the properties and the number of soil types in the soil profile, and the global equilibrium between the soil layers and the loaded pile. An iterative process is performed to satisfy the equilibrium between the mobilized geometry of the passive wedge of the layered soil and the deflected pattern of the pile for any level of loading.

While the shape of the wedge in any soil layer depends upon the properties of that layer and, therefore, satisfies the nature of a Winkler foundation of independent "soil" springs in BEF analysis, realize that there is forced interdependence given that all components of the compound wedge have the same depth (h) in common. Therefore, the mobilized depth (h) of the compound wedge at any time is a function of the various soils (and their stress levels), the bending stiffness (EI), and head fixity conditions (fixed, free, or other) of the pile. In fact, the developing depth of the compound wedge can be thought of as a retaining wall of changing height, h . Therefore, the resultant "soil" reaction, p , from any soil layer is really a "soil-pile" reaction that depends upon

the neighboring soil layers and the pile properties as they, in turn, influence the current depth, h . In other words, the p - y response of a given soil layer is not unique. The governing equations of the mobilized passive wedge shape are applied within each one- or two-foot sublayer i (of a given soil layer I) and can be written as follows:

$$(\Theta_m)_i = 45 - \frac{(\mathbf{j}_m)_i}{2} \quad (5-6)$$

$$(\mathbf{b}_m)_i = 45 + \frac{(\mathbf{j}_m)_i}{2} \quad (5-7)$$

$$\left(\overline{BC}\right) = D + (h - x_i) 2 (\tan \mathbf{b}_m)_i (\tan \mathbf{j}_m)_i \quad (5-8)$$

where h symbolizes the entire depth of the compound passive wedge in front of the pile and x_i represents the depth from the top of the pile or compound passive wedge to the middle of the sublayer under consideration. Equations 5-6 through 5-8 are applied at the middle of each sublayer. In the case of short and intermediate shafts, x_i is measured downward from the point of zero crossing and replaces the term $(h - x_i)$ in Eqn 5-8, as shown in Fig. 5-6, for analysis of the lower wedge.

5.5 SOIL STRESS-STRAIN RELATIONSHIP

The horizontal strain (ϵ) in the soil in the passive wedge in front of the pile is the predominant parameter in the SW model; hence, the name “strain wedge”. Consequently, the horizontal stress change ($\Delta\sigma_h$) is constant across the width of the rectangle BCLM (of face width \overline{BC} of the passive wedge), as shown in Fig. 5-4. The stress-strain relationship is defined based on the results of the isotropically consolidated drained (sand) or undrained (clay) triaxial test. These properties are summarized as follows:

- The major principle stress change ($\Delta\sigma_h$) in the wedge is in the direction of pile movement, and it is equivalent to the deviatoric stress in the triaxial test as shown in Fig. 5-4 (assuming that the horizontal direction in the field is taken as the axial direction in the triaxial test).
- The vertical stress change ($\Delta\sigma_v$) and the perpendicular horizontal stress change ($\Delta\sigma_{ph}$) equal zero, corresponding to the standard triaxial compression test where deviatoric stress

is increased while confining pressure remains constant.

- The initial horizontal effective stress is taken as

$$\bar{\mathbf{s}}_{ho} = K \bar{\mathbf{s}}_{vo} = \bar{\mathbf{s}}_{vo}$$

where $K=1$ due to pile installation effects. Therefore, the isotropic confining pressure in the triaxial test is taken as the vertical effective stress ($\bar{\sigma}_{vo}$) at the associated depth.

- The horizontal stress change in the direction of pile movement is related to the current level of horizontal strain (ϵ) and the associated Young's modulus in the soil, as are the deviatoric stress and the axial strain, to the secant Young's modulus ($E = \Delta\sigma_h/\epsilon$) in the triaxial test.
- Both the vertical strain (ϵ_v) and the horizontal strain perpendicular to pile movement (ϵ_{ph}) are equal and are given as

$$\epsilon_v = \epsilon_{ph} = -\nu\epsilon$$

where ν is the Poisson's ratio of the soil.

It can be demonstrated from a Mohr's circle of soil strain, as shown in Fig. 5-10, that shear strain, γ , is defined as

$$\frac{\mathbf{g}}{2} = \frac{1}{2} (\mathbf{e} - \mathbf{e}_v) \sin 2\Theta_m = \frac{1}{2} \mathbf{e} (1 + \mathbf{n}) \sin 2\Theta_m \quad (5-9)$$

The corresponding stress level (SL) in sand (see Fig. 5-11) is

$$SL = \frac{\Delta \mathbf{s}_h}{\Delta \mathbf{s}_{hf}} = \frac{\tan^2 \left(45 + \frac{\mathbf{j}_m}{2} \right) - 1}{\tan^2 \left(45 + \frac{\mathbf{j}}{2} \right) - 1} \quad (5-10)$$

where the horizontal stress change at failure (or the deviatoric stress at failure in the triaxial test) is

$$\Delta \mathbf{s}_{hf} = \bar{\mathbf{s}}_{vo} \left[\tan^2 \left(45 + \frac{\mathbf{j}}{2} \right) - 1 \right] \quad (5-11)$$

In clay,

$$SL = \frac{\Delta \mathbf{s}_h}{\Delta \mathbf{s}_{hf}} ; \quad \Delta \mathbf{s}_{hf} = 2 S_u \quad (5.12)$$

where S_u represents the undrained shear strength which may vary with depth. Determination of the values of SL and ϕ_m in clay requires the involvement of an effective stress analysis which is presented later in this chapter.

The relationships above show clearly that the passive wedge response and configuration change with the change of the mobilized friction angle (ϕ_m) or stress level (SL) in the soil. Such behavior provides the flexibility and the accuracy for the strain wedge model to accommodate both small and large strain cases. The above equations are applied for each soil sublayer along the shaft in order to evaluate the varying stress level in the soil and the geometry of the passive wedges.

A power function stress-strain relationship is employed in SW model analysis for both sand and clay soils. It reflects the nonlinear variation in stress level (SL) with axial strain (ϵ) for the condition of constant confining pressure. To be applicable over the entire range of soil strain, it takes on a form that varies in stages as shown in Fig. 5-12. The advantage of this technique is that it allows the three stages of horizontal stress, described in the next section, to occur simultaneously in different sublayers within the passive wedge.

5.5.1 Horizontal Stress Level (SL)

Stage I ($\epsilon \leq \epsilon_{50\%}$)

The relationship between stress level and strain at each sublayer (i) in the first stage is assessed using the following equation,

$$SL_i = \frac{\mathbf{l}_i \mathbf{e}}{(\mathbf{e}_{50})_i} \exp(-3.707 SL_i) \quad (5.13)$$

where 3.707 and λ ($\lambda = 3.19$) represent the fitting parameters of the power function relationship, and ϵ_{50} symbolizes the soil strain at 50 percent stress level at the associated confining pressure.

Stage II ($e_{50\%} \leq e \leq e_{80\%}$)

In the second stage of the stress-strain relationship, Eqn. 5.13 is still applicable. However, the value of the fitting parameter λ is taken to vary in a linear manner with SL from 3.19 at the 50 percent stress level to 2.14 at the 80 percent stress level as shown in Fig. 5-12b.

Stage III ($e \geq e_{80\%}$)

This stage represents the final loading zone which extends from 80 percent to 100 percent stress level. The following equation is used to assess the stress-strain relationship in this range,

$$SL_i = \exp \left[\ln 0.2 + \frac{100 e_i}{(m e_i + q_i)} \right] ; \quad SL_i \geq 0.80 \quad (5-14)$$

where $m=59.0$ and $q=95.4 \epsilon_{50}$ are the required values of the fitting parameters.

The three stages mentioned above are developed based on unpublished experimental results (Norris 1977). In addition, the continuity of the stress-strain relationship is maintained along the SL- ϵ curve at the merging points between the mentioned stages.

As shown in Fig. 5-13, if ϵ_{50} of the soil is constant with depth (x), then, for a given horizontal strain (ϵ), SL from Eqns 5-13 or 5-14 will be constant with x . On the other hand, since strength, $\Delta\sigma_{hf}$, varies with depth (e.g., see Eqns. 5-11 and 5-12), $\Delta\sigma_h (= SL \Delta\sigma_{hf})$ will vary in a like fashion. However, ϵ_{50} is affected by confining pressure ($\bar{\sigma}_{v0}$) in sand and S_u in clay. Therefore, SL for a given ϵ will vary somewhat with depth.

The Young's modulus of the soil from both the shear loading phase of the triaxial test and the strain wedge model is

$$E_i = \frac{(\Delta s_h)_i}{e} = \frac{SL_i (\Delta s_{hf})_i}{e} \quad (5.15)$$

It can be seen from the previous equations that stress level, strain and Young's modulus at each sublayer (i) depend on each other, which results in the need for an iterative solution technique to satisfy the equilibrium between the three variables.

5.6 SHEAR STRESS ALONG THE PILE SIDES (SL_t)

Shear stress (τ) along the pile sides in the SW model (see Fig. 5-4) is defined according to the soil type (sand or clay).

5.6.1 Pile Side Shear in Sand

In the case of sand, the shear stress along the pile sides depends on the effective stress ($\bar{\sigma}_{vo}$) at the depth in question and the mobilized angle of friction between the sand and the pile (ϕ_s). The mobilized side shear depends on the stress level and is given by the following equation,

$$t_i = (\bar{\sigma}_{vo})_i \tan(\mathbf{j}_s)_i; \quad \text{where} \quad \tan(\mathbf{j}_s)_i = 2 \tan(\mathbf{j}_m)_i \quad (5-16)$$

In Eqn. 5-16, note that mobilized side shear angle, $\tan\phi_s$, is taken to develop at twice the rate of the mobilized friction angle ($\tan\phi_m$) in the mobilized wedge. Of course, ϕ_s is limited to the fully developed friction angle (ϕ) of the soil.

5.6.2 Pile Side Shear Stress in Clay

The shear stress along the pile sides in clay depends on the clay's undrained shear strength. The stress level of shear along the pile sides (SL_t) differs from that in the wedge in front of the pile. The side shear stress level is function of the shear movement, equal to the pile deflection (y) at depth x from the ground surface. This implies a connection between the stress level (SL) in the wedge and the pile side shear stress level (SL_t). Using the Coyle-Reese (1966) "t-z" shear stress transfer curves (Fig. 5-14), values for SL_t can be determined. The shear stress transfer curves represent the relationship between the shear stress level experienced by a one-foot diameter pile embedded in clay with a peak undrained strength, S_u , and side resistance, τ_{ult} (equal to ζ times the adhesional strength αS_u), for shear movement, y. The shear stress load transfer curves of Coyle-Reese can be normalized by dividing curve A ($0 < x < 3$ m) by $\zeta = 0.53$, curve B ($3 < x <$

6 m) by $\zeta = 0.85$, and curve C ($x > 6$ m) by $\zeta = 1.0$. These three values of normalization (0.53, 0.85, 1.0) represent the peaks of the curves A, B, and C, respectively, in Fig. 5-15a. Figure 5-15b shows the resultant normalized curves. Knowing pile deflection (y), one can assess the value of the mobilized pile side shear stress (τ) as

$$\mathbf{t}_i = (SL_t)_i (\mathbf{t}_{ult})_i \quad (5-17)$$

where

$$(\mathbf{t}_{ult})_i = \mathbf{z}(\alpha S_u)_i \quad (5-18)$$

and α indicates the adhesion value after Tomlinson (1957).

The normalized shear stress load transfer curves can be represented by the following equations.

For the normalized curves A ($x < 3$ m) and B ($3 < x < 6$ m),

$$SL_t = 12.9 y D - 40.5 y^2 D^2 \quad (5-19)$$

For the normalized curve C ($x > 6$ m)

$$SL_t = 32.3 y D - 255 y^2 D^2 \quad (5-20)$$

where y is in cm and D in m.

From the discussion above, it is obvious that SL_t varies nonlinearly with the pile deflection, y , at a given soil depth, x . Also, SL_t changes nonlinearly with soil depth for a given value of soil displacement/strain (see Fig. 5-15). These concepts are employed in each sublayer of clay.

5.7 SOIL PROPERTY CHARACTERIZATION IN THE STRAIN WEDGE MODEL

One of the main advantages of the SW model approach is the simplicity of the required soil properties necessary to analyze the problem of a laterally loaded pile. The properties required represent the basic and the most common properties of soil, such as the effective unit weight and the angle of internal friction or undrained strength.

The soil profile is divided into one or two foot sublayers, and each sublayer is treated as an independent entity with its own properties. In this fashion, the variation in soil properties or response (such as ϵ_{50} and ϕ in the case of sand, or S_u and $\bar{\phi}$ in the case of clay) at each sublayer of soil can be explored. It is obvious that soil properties should not be averaged at the midheight of the passive wedge in front of the pile for a uniform soil profile (as in the earlier work of Norris 1986), or averaged for all sublayers of a single uniform soil layer of a multiple layer soil profile.

5.7.1 Properties Employed for Sand Soil

- Effective unit weight (total above water table, buoyant below), $\bar{\gamma}$
- Void ratio, e , or relative density, D_r
- Angle of internal friction, ϕ
- Soil strain at 50% stress level, ϵ_{50}

While standard subsurface exploration techniques and available correlations may be used to evaluate or estimate $\bar{\gamma}$, e or D_r , and ϕ , some guidance may be required to assess ϵ_{50} .

The ϵ_{50} represents the axial strain (ϵ_1) at a stress level equal to 50 percent in the ϵ_1 -SL relationship that would result from a standard drained (CD) triaxial test. The confining (consolidation) pressure for such tests should reflect the effective overburden pressure ($\bar{\sigma}_{vo}$) at the depth (x) of interest. The ϵ_{50} changes from one sand to another and also changes with density state. In order to obtain ϵ_{50} for a particular sand, one can use the group of curves shown in Fig. 5-16 (Norris 1986) which show a variation based upon the uniformity coefficient, C_u , and void ratio, e . These curves have been assessed from sand samples tested with “frictionless” ends in CD tests at a confining pressure equal to 42.5 kPa (Norris 1977). Since the confining pressure changes with soil depth, ϵ_{50} , as obtained from Fig. 5-16, should be modified to match the existing pressure as follows:

$$\left(\epsilon_{50} \right)_i = \left(\epsilon_{50} \right)_{42.5} \left(\frac{\bar{\sigma}_{vo}_i}{42.5} \right)^{0.2} \quad (5-21)$$

$$(\Delta \mathbf{s}_{hf})_i = (\bar{\mathbf{s}}_{vo})_i \left[\tan^2 \left(45 + \frac{\bar{\mathbf{j}}_i}{2} \right) - 1 \right] \quad (5-22)$$

where $\bar{\sigma}_{vo}$ should be in kPa.

5.7.2 The Properties Employed for Clay

- Effective unit weight $\bar{\gamma}$
- Plasticity index, PI
- Effective angle of friction, $\bar{\phi}$
- Undrained shear strength, S_u
- Soil strain at 50% stress level, ϵ_{50}

Plasticity index, PI, and undrained shear strength, S_u , are considered the governing properties because the effective angle of internal friction, $\bar{\phi}$, can be estimated from the PI based on Fig. 5-17. The ϵ_{50} from an undrained triaxial test (UU at depth x or CU with $\sigma_3 = \bar{\sigma}_{vo}$) can be estimated based on S_u as indicated in Fig. 5-18.

An effective stress (ES) analysis is employed with clay soil as well as with sand soil. The reason behind using the ES analysis with clay, which includes the development of excess porewater pressure with undrained loading, is to define the three-dimensional strain wedge geometry based upon the more appropriate effective stress friction angle, $\bar{\phi}$. The relationship between the normally consolidated clay undrained shear strength, S_u , and $\bar{\sigma}_{vo}$ is taken as

$$S_u = 0.33 \bar{\mathbf{s}}_{vo} \quad (5-23)$$

assuming that S_u is the equivalent undrained standard triaxial test strength. The effective stress analysis relies upon the evaluation of the developing excess porewater pressure based upon Skempton's equation (1954), i.e.

$$\Delta u = B \left[\Delta \mathbf{s}_3 + A_u (\Delta \mathbf{s}_1 - \Delta \mathbf{s}_3) \right] \quad (5-24)$$

where B equals 1 for saturated soil. Accordingly,

$$\Delta u = \Delta \mathbf{s}_3 + A_u (\Delta \mathbf{s}_1 - \Delta \mathbf{s}_3) \quad (5-25)$$

Note that $\Delta \sigma_3 = 0$ both in the shear phase of the triaxial test and in the strain wedge. Therefore, the mobilized excess porewater pressure is

$$\Delta u = A_u \Delta \mathbf{s}_1 \quad (5-26)$$

where $\Delta \sigma_1$ represents the deviatoric stress change in the triaxial test and $\Delta \sigma_h$ in the field, i.e.

$$\Delta u = A_u \Delta \mathbf{s}_h \quad (5-27)$$

Therefore, using the previous relationships, the Skempton equation can be rewritten for any sublayer (i) as follows:

$$(\Delta u)_i = (A_u)_i SL_i (\Delta \mathbf{s}_{hf})_i = (A_u)_i SL_i 2 (S_u)_i \quad (5-28)$$

The initial value of parameter A_u is 0.333 and occurs at very small strain for elastic soil response. In addition, the value of parameter A_{uf} that occurs at failure at any sublayer (i) is given by the following relationship

$$(A_{uf})_i = \frac{1}{2} \left(1 + \frac{1/(S_u)_i}{(\bar{\mathbf{s}}_{vo})_i \sin \bar{\mathbf{j}}_i} \right) \quad (5-29)$$

after Wu (1966) as indicated in Fig. 5-19.

In Eqn. 5.29, $\bar{\varphi}$ symbolizes the effective stress angle of internal friction; and, based on Eqn. 5-23, $S_u/\bar{\sigma}_{vo}$ equals 0.33. However, A_u is taken to change with stress level in a linear fashion as

$$(A_u)_i = 0.333 + SL_i [(A_{uf})_i - 0.333] \quad (5-30)$$

By evaluating the value of A_u , one can effectively calculate the excess porewater pressure, and then can determine the value of the effective horizontal stress, $(\bar{\sigma}_{vo} + \Delta\sigma_h - \Delta u)$, and the effective confining pressure, $(\bar{\sigma}_{vo} - \Delta u)$ at each sublayer, as shown in Fig. 5-19. Note that the mobilized effective stress friction angle, $\bar{\phi}_m$, can be obtained from the following relationship.

$$\tan^2 \left(45 + \frac{(\bar{j}_m)_i}{2} \right) = \frac{(\bar{s}_{vo} + \Delta s_h - \Delta u)_i}{(\bar{s}_{vo} - \Delta u)_i} \quad (5-31)$$

The targeted values of $\bar{\phi}_{mi}$ and SL_i in a clay sublayer and at a particular level of strain (ϵ) can be obtained by using an iterative solution that includes Eqns 5-12 through 5-14, and 5-28 through 5-31.

5.8 SOIL-PILE INTERACTION IN THE STRAIN WEDGE MODEL

The strain wedge model relies on calculating the modulus of subgrade reaction, E_s , which reflects the soil-pile interaction at any level of soil strain during pile loading. E_s also represents the secant slope at any point on the p-y curve, i.e.

$$E_s = \frac{p}{y} \quad (5-32)$$

Note that p represents the force per unit length of the pile or the BEF soil-pile reaction, and y symbolizes the pile deflection at that soil depth. In the SW model, E_s is related to the soil's Young's modulus, E, by two linking parameters, A and ψ_s . It should be mentioned here that the SW model establishes its own E_s from the Young's modulus of the strained soil, and therefore, one can assess the p-y curve using the strain wedge model analysis. Therefore, E_s should first be calculated using the strain wedge model analysis to identify the p and y values.

Corresponding to the horizontal slice (a soil sublayer) of the passive wedge at depth x (see Figs. 5-2 and 5-4), the horizontal equilibrium of horizontal and shear stresses is expressed as

$$p_i = (\Delta s_h)_i \overline{BC}_i S_1 + 2 t_i D S_2 \quad (5-33)$$

where S_1 and S_2 equal to 0.75 and 0.5, respectively, for a circular pile cross section, and equal to 1.0 each for a square pile (Briaud et al. 1984). Alternatively, one can write the above equation as follows:

$$A_i = \frac{p_i / D}{(\Delta \mathbf{s}_h)_i} = \frac{\overline{BC}_i S_1}{D} + \frac{2 \mathbf{t}_i S_2}{(\Delta \mathbf{s}_h)_i} \quad (5-34)$$

where A symbolizes the ratio between the equivalent pile face stress, p/D , and the horizontal stress change, $\Delta \sigma_h$, in the soil. (In essence, it is the multiplier that, when taken times the horizontal stress change, gives the equivalent face stress.) From a different perspective, it represents a normalized width (that includes side shear and shape effects) that, when multiplied by $\Delta \sigma_h$ yields p/D . By combining the equations of the passive wedge geometry and the stress level with the above relationship, one finds that

$$A_i = S_1 \left(1 + \frac{(h - x_i) 2 (\tan \mathbf{b}_m \tan \mathbf{j}_m)_i}{D} \right) + \frac{2 S_2 (\overline{\mathbf{s}}_{vo})_i (\tan \mathbf{f}_s)_i}{(\Delta \mathbf{s}_h)_i} \quad \text{in sand} \quad (5-35)$$

$$A_i = S_1 \left(1 + \frac{(h - x_i) 2 (\tan \mathbf{b}_m \tan \overline{\mathbf{j}}_m)_i}{D} \right) + \frac{S_2 (SL_t)_i}{SL_i} \quad \text{in clay} \quad (5-36)$$

Here the parameter A is a function of pile and wedge dimensions, applied stresses, and soil properties. However, given that $\Delta \sigma_h = E \epsilon$ in Eqn. 2.33,

$$p_i = A_i D (\Delta \mathbf{s}_h)_i = A_i D E_i \mathbf{e} \quad (5-37)$$

For the upper passive wedge, ϵ represents the uniform soil strain and is replaced by ϵ_x for soil sublayers of the lower passive wedge. The second linking parameter, Ψ_s , relates the soil strain in the SW model to the linearized pile deflection angle, δ . Referring to the normalized pile deflection shape shown in Figs. 5-3 and 5-5

$$\mathbf{d} = \frac{\mathbf{g}}{2} \quad (5-38)$$

$$\frac{\mathbf{g}}{2} = \frac{\mathbf{g}_{\max}}{2} \sin 2 \Theta_m \quad (5-39)$$

and

$$\frac{\mathbf{g}_{\max}}{2} = \frac{\mathbf{e} - \mathbf{e}_v}{2} = \frac{(1 + \mathbf{n}) \mathbf{e}}{2} \quad (5-40)$$

where γ denotes the shear strain in the developing passive wedge. Using Eqns. 5-39 and 5.40, Eqn. 5-38 can be rewritten as

$$\mathbf{d} = \frac{\mathbf{e}(1 + \mathbf{n}) \sin 2 \Theta_m}{2} \quad (5-41)$$

Based on Eqn. 5-41, the relationship between ε and δ can expressed as

$$\Psi = \frac{\mathbf{e}}{\mathbf{d}} \quad (5-42)$$

or

$$\Psi = \frac{2}{(1 + \mathbf{n}) \sin 2 \Theta_m} \quad (5-43)$$

The parameter ψ varies with the Poisson's ratio of the soil and the soil's mobilized angle of internal friction (φ_m) and the mobilized passive wedge angle (Θ_m).

Poisson's ratio for sand can vary from 0.1 at a very small strain to 0.5 or larger (due to dilatancy) at failure, while the base angle, Θ_m , can vary between 45° (for $\varphi_m = 0$ at $\varepsilon = 0$) and 25° (for, say, $\varphi_m = 40^\circ$ at failure), respectively. For this range in variation for ν and φ_m , the parameter Ψ for sand varies between 1.81 and 1.74 with an average value of 1.77. In clay soil, Poisson's ratio is assumed to be 0.5 (undrained behavior) and the value of the passive wedge base angle, Θ_m , can vary between 45° (for $\varphi_m = 0$ at $\varepsilon = 0$) and 32.5° (for, say, $\overline{\varphi}_m = 25^\circ$ at failure). Therefore, the value of the parameter ψ will vary from 1.47 to 1.33, with an average value of 1.4.

It is clear from the equations above that employing the multi-sublayer technique greatly influences the values of soil-pile interaction as characterized by the parameter, A_i , which is

affected by the changing effective stress and soil strength from one sublayer to another. The final form of the modulus of subgrade reaction can be expressed as

$$(E_s)_i = \frac{p_i}{y_i} = \frac{A_i D e E_i}{\mathbf{d}(h - x_i)} = \frac{A_i}{(h - x_i)} D \Psi E_i \quad (5-44)$$

It should be mentioned that the SW model develops its own set of non-unique p-y curves which are function of both soil and pile properties, and are affected by soil continuity (layering) as presented by Ashour et al. (1996). For the lower passive wedge, $(h - x_i)$ will be replaced by x_i that is measured downward from the point of zero crossing (Fig. 5-6).

5.9 PILE HEAD DEFLECTION

As mentioned previously, the deflection pattern of the pile in the SW model is continuous and linear. Based on this concept, pile deflection can be assessed using a simplified technique which provides an estimation for the linearized pile deflection, especially y_o at the pile head. By using the multi-sublayer technique, the deflection of the pile can be calculated starting with the base of the mobilized passive wedge and moving upward along the pile, accumulating the deflection values at each sublayer as shown in the following relationships and Fig. 5-20.

$$y_i = H_i \mathbf{d}_i = H_i \frac{e}{\Psi_s} \quad (5-45)$$

$$y_o = \sum y_i \quad i = 1 \text{ to } n \quad (5-46)$$

where the Ψ_s value changes according to the soil type (sand or clay), and H_i indicates the thickness of sublayer i and n symbolizes the current number of sublayers in the mobilized passive wedge.

The main point of interest is the pile head deflection which is a function of not only the soil strain but also of the depth of the compound passive wedge that varies with soil and pile properties and the level of soil strain.

5.10 ULTIMATE RESISTANCE CRITERIA IN STRAIN WEDGE MODEL

The mobilized passive wedge in front of a laterally loaded pile is limited by certain constraint criteria in the SW model analysis. Those criteria differ from one soil to another and are applied to each sublayer. Ultimate resistance criteria govern the shape and the load capacity of the wedge in any sublayer in SW model analysis. The progressive development of the ultimate resistance with depth is difficult to implement without employing the multi- sublayer technique.

5.10.1 Ultimate Resistance Criterion of Sand Soil

The mobilization of the passive wedge in sand soil depends on the horizontal stress level, SL , and the pile side shear resistance, τ . The side shear stress is a function of the mobilized side shear friction angle, ϕ_s , as mentioned previously, and reaches its ultimate value ($\phi_s = \phi$) earlier than the mobilized friction angle, ϕ_m , in the wedge (i.e. $SL_i \geq SL$). This causes a decrease in the rate of growth of sand resistance and the fanning of the passive wedge as characterized by the second term in Eqns 5-33 and 5-35, respectively.

Once the stress level in the soil of a sublayer of the wedge reaches unity ($SL_i = 1$), the stress change and wedge fan angle in that sublayer cease to grow. However, the width \overline{BC} of the face of the wedge can continue to increase as long as ϵ (and, therefore, h in Eqn. 5-8) increases. Consequently, soil-pile resistance, p , will continue to grow more slowly until a condition of initial soil failure ($SL_i = 1$) develops in that sublayer. At this instance, $p = p_{ult}$ where p_{ult} in sand, given as

$$(p_{ult})_i = (\Delta s_{hf})_i \overline{BC}_i S_1 + 2(t_f)_i D S_2 \quad (5.47)$$

p_{ult} is “a temporary” ultimate condition, i.e. the fanning angle of the sublayer is fixed and equal to ϕ_i , but the depth of the passive wedge and, hence, \overline{BC} continue to grow. The formulation above reflects that the near-surface “failure” wedge does not stop growing when all such sublayers reach their ultimate resistance at $SL = 1$ because the value of h at this time is not limited. Additional load applied at the pile head will merely cause the point at zero deflection and, therefore, h to move down the pile. More soil at full strength ($SL = 1$) will be mobilized to

the deepening wedge as BC, therefore, p_{ult} will increase until either flow around failure or a plastic hinge in the pile occurs.

Recognize that flow around failure occurs in any sublayer when it is easier for the sand at that depth to flow around the pile in a local bearing capacity failure than for additional sand to be brought to failure and added to the already developed wedge. However, the value at which flow failure occurs [$A_i = (A_{ult})_i$, $(p_{ult})_i = (\Delta\sigma_{hf})_i (A_{ult})_i D$] in sand is so large that it is not discussed here. Alternatively, a plastic hinge can develop in the pile when the pile material reaches its ultimate resistance at a time when $SL_i \leq 1$ and $A_i < (A_{ult})_i$. In this case, h becomes fixed, and \overline{BC}_i and p_i will be limited when SL_i becomes equal to 1.

5.10.2 Ultimate Resistance Criterion of Clay Soil

The situation in clay soil differs from that in sand and is given by Gowda (1991) as a function of the undrained strength $(S_u)_i$ of the clay sublayer.

$$(p_{ult})_i = 10(S_u)_i D S_1 + 2(S_u)_i D S_2 \quad (5-48)$$

Consequently,

$$(A_{ult})_i = \frac{(p_{ult})_i}{(\Delta\sigma_{hf})_i} = \frac{(p_{ult})_i}{D 2(S_u)_i} = 5 S_1 + S_2 \quad (5-49)$$

A_{ult} indicates the limited development of the sublayer wedge geometry for eventual development of flow around failure ($SL_i = 1$) and, consequently, the maximum fanning angle in that sublayer becomes fixed, possibly at a value $\phi_m \leq \overline{\phi}$. If a plastic hinge develops in the pile at SL_i less than 1, then h will be limited, but \overline{BC}_i , and p_i will continue to grow until A_i is equal to A_{ult} or p_i is equal to $(p_{ult})_i$.

5.11 VERTICAL SIDE SHEAR RESISTANCE

As seen in Fig. 5-21, the vertical side shear stress distribution around the shaft cross section is assumed to follow a cosine function. It is assumed that there is no contact (active pressure) on the backside of the shaft due to the lateral deflection. The peak (q) of side shear stress develops at angle $\theta = 0$ and decreases to zero at angle $\theta = 90^\circ$. The total vertical side shear force (V_v) induced along a unit length of the shaft is expressed as

$$V_v = 2 \int_0^{p/2} q r \cos \mathbf{q} \, d\mathbf{q} = 2q (r \sin \mathbf{q})_0^{p/2} = Dq \quad (5-50)$$

and the induced moment (M_{x-x}) per unit length of the shaft is given as

$$\begin{aligned} M_{x-x} &= 2 \int_0^{p/2} (q r \cos \mathbf{q} \, d\mathbf{q}) (r \cos \mathbf{q}) = 2qr^2 \int_0^{p/2} \cos^2 \mathbf{q} \, d\mathbf{q} \\ &= 2qr^2 \int_0^{p/2} \frac{1}{2} (\cos 2\mathbf{q} + 1) \, d\mathbf{q} \\ &= qr^2 \int_0^{p/2} (\cos 2\mathbf{q} + 1) \, d\mathbf{q} \\ &= qr^2 \left(\frac{1}{2} (\sin 2\mathbf{q} + \mathbf{q}) \right)_0^{p/2} = \frac{q D^2 p}{8} \end{aligned} \quad (5-51)$$

M_{x-x} represents the term M_R in Eqn. 5-1.

5.12 SHAFT BASE RESISTANCE

The soil shear resistance at the base of the shaft (V_b) that is shown in Fig. 5-1 is a function of the soil shear stress (τ_b) induced at the contact surface between the soil and shaft base. The shear stress (τ_b) varies with lateral deflection of the shaft base and the axial load delivered at the shaft base. Based on the failure mechanism at the shaft base for sand and clay that are presented in Chapter 3 and 4, Fig. 5-22 shows the shear stress (τ_b) that develops at the shaft base embedded in sand or clay soil. Unlike the clay case, the ultimate shear resistance at the base of the shaft increases with the axial load carried by the shaft base (Figs. 4-1 and 5-22).

The shear resistance at the shaft base can be determined as follows,

1. Using the lateral deflection at the shaft base (y_b) that is obtained from the lateral shaft analysis with no shaft base resistance, the soil shear strain at the base (γ_b) is calculated as,

$$\mathbf{g}_b = \frac{y_b}{2D} \quad (5-52)$$

where D is the shaft diameter, and the effective depth of the shear deformation is assumed to be equal to $2D$

2. In the first step of analysis, assume the normal strain (ϵ_b) equal to the shear strain (γ_b). Based on the normal stress strain relationship presented in Section 5.5.1, the stress level (SL) can be evaluated and the associated Poisson's ratio (ν) is calculated as follows,

$$\mathbf{n} = 0.1 + 0.4SL \quad (5-53)$$

It should be noted the $\Delta\sigma_{hf}$ used in Eqns. 5-10 through 5-12 is constant with clay ($\Delta\sigma_{hf} = 2S_u$) and varies with the load carried by the shaft base in the case of sand (Figs. 4-1 and 5-22), i.e.

$$\Delta\mathbf{s}_{hf} = (\bar{\mathbf{s}}_3)_{IV} \left[\tan^2 \left(45 + \frac{\mathbf{j}}{2} \right) - 1 \right] \quad (5-54)$$

In sand soil, the increase of the shaft base load ($F_b = 0.6 q_{net} A_b = \sigma_d A_b = SL \Delta\sigma_{hf} A_b$) results in the increase of the accompanying confining pressure $(\bar{\mathbf{s}}_3)_{IV}$.

3. The induced normal strain (ϵ_b) is recalculated as follows,

$$\mathbf{e}_b = \frac{\mathbf{g}_b}{(1 + \mathbf{n})} \quad (5-55)$$

4. Repeat steps 2 and 3 to refine the value of ϵ_b by averaging the new and old values of ϵ_b until reaching the desired convergence.
5. Compute the associated soil shear stress that develops on the shaft base (τ_b) as follows:

$$\mathbf{t}_b = SL S_u \quad (\text{Clay}) \quad (5-56a)$$

$$\mathbf{t}_b = 0.5 SL \Delta \mathbf{s}_{bf} \quad (\text{Sand}) \quad (5-56b)$$

$$V_b = \mathbf{t}_b A_b \quad (5-57)$$

where F_b and V_b are the axial load (as calculated in Chapter 4) and the shear resistance carried by the shaft base.

6. Analyze the laterally loaded shaft as a Beam on Elastic Foundations (Section 5-13) considering the effect of the base resistance. The base shear resistance is evaluated in each trial according to the lateral deflection induced at the shaft base.

5.13 STABILITY ANALYSIS IN THE STRAIN WEDGE MODEL

The objective of the SW model is to establish the soil response as well as model the soil-pile interaction through the modulus of subgrade reaction, E_s . The shape and the dimensions of the passive wedge in front of the pile basically depend on two types of stability which are the local stability of the soil sublayer and the global stability of the pile and the passive wedge. However, the global stability of the passive wedge depends, in turn, on the local stability of the soil sublayers.

5.13.1 Local Stability of a Soil Sublayer in the Strain Wedge Model

The local stability analysis in the strain wedge model satisfies equilibrium and compatibility among the pile segment deflection, soil strain, and soil resistance for the soil sublayer under consideration. Such analysis allows the correct development of the actual horizontal stress change, $\Delta\sigma_h$, pile side shear stress, τ , and soil-pile reaction, p , associated with that soil sublayer (see Figs. 5-2 and 5-4). It is obvious that the key parameters of local stability analysis are soil strain, soil properties, and pile properties.

5.13.2 Global Stability in the Strain Wedge Model

The global stability, as analyzed by the strain wedge model, satisfies the general compatibility among soil reaction, pile deformations, and pile stiffness along the entire depth of the developing passive wedge in front of the pile. Therefore, the depth of the passive wedge depends on the

global equilibrium between the loaded pile and the developed passive wedge. This requires a solution for Eqn. 5-1.

The global stability is an iterative beam on elastic foundation (BEF) problem that determines the correct dimensions of the passive wedge, the corresponding straining actions (deflection, slope, moment, and shear) in the pile, and the external loads on the pile. Satisfying global stability conditions is the purpose of linking the three-dimensional strain wedge model to the BEF approach. The major parameters in the global pile stability problem are pile stiffness, EI , and the modulus of subgrade reaction profile, E_s , as determined from local stability in the strain wedge analysis. Since these parameters are determined for the applied soil strain, the stability problem is no longer a soil interaction problem but a one-dimensional BEF problem. Any available numerical technique, such as the finite element or the finite difference method, can be employed to solve the global stability problem. The modeled problem, shown in Fig. 5-8c, is a BEF and can be solved to identify the depth, X_o , of zero pile deflection.

5.14 SUMMARY

The SW model approach presented here provides an effective method for solving the problem of a laterally loaded pile/shaft in layered soil. This approach assesses its own nonlinear variation in modulus of subgrade reaction or p-y curves. The SW model allows the assessment of the nonlinear p-y curve response of a laterally loaded pile based on the envisioned relationship between the three-dimensional response of a flexible pile in the soil to its one-dimensional beam on elastic foundation parameters. In addition, the SW model employs stress-strain-strength behavior of the soil as established from the triaxial test in an effective stress analysis to evaluate mobilized soil behavior.

The SW model accounts for the vertical side shear resistance that develops effectively with large diameter shafts. Such resistance enhances the performance of the large diameter shafts and increases with progressive lateral deflection. The evaluation of the vertical side shear resistance is based on the assessed t-z curve and affects the shape of the predicted p-y curve. The formulations of the t-z curve presented in Chapters 3 and 4 are employed in the SW model analysis and coupled with the shaft deformations.

Compared to empirically based approaches which rely upon a limited number of field tests, the SW approach depends on well known or accepted principles of soil mechanics (the stress-strain-strength relationship) in conjunction with effective stress analysis. Moreover, the required parameters to solve the problem of the laterally loaded pile are a function of basic soil properties that are typically available to the designer.

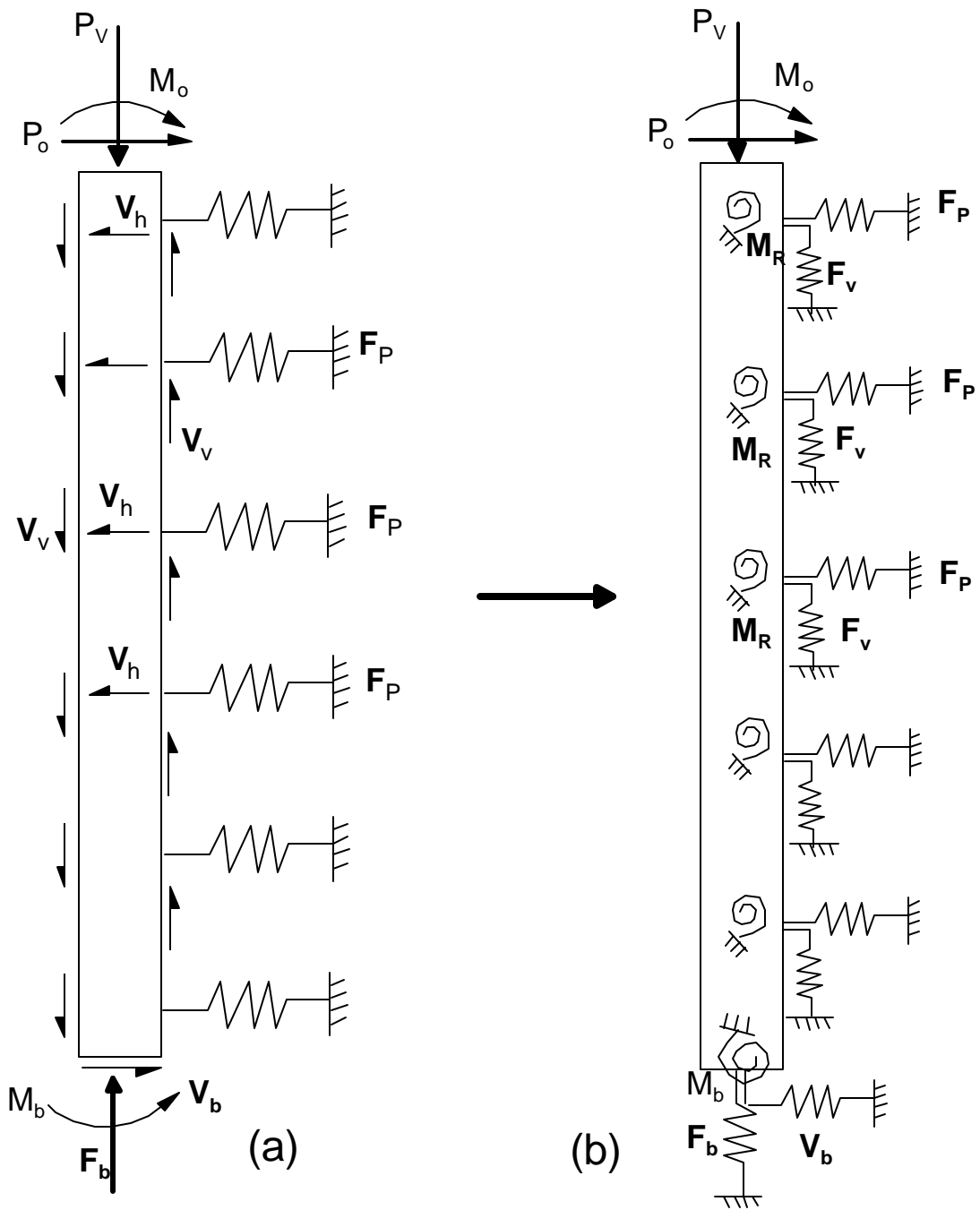


**Fig. 5-1 Characterization of Large Diameter Long, Intermediate or Short Shafts
In Terms of a) Forces and b) Nonlinear Springs**

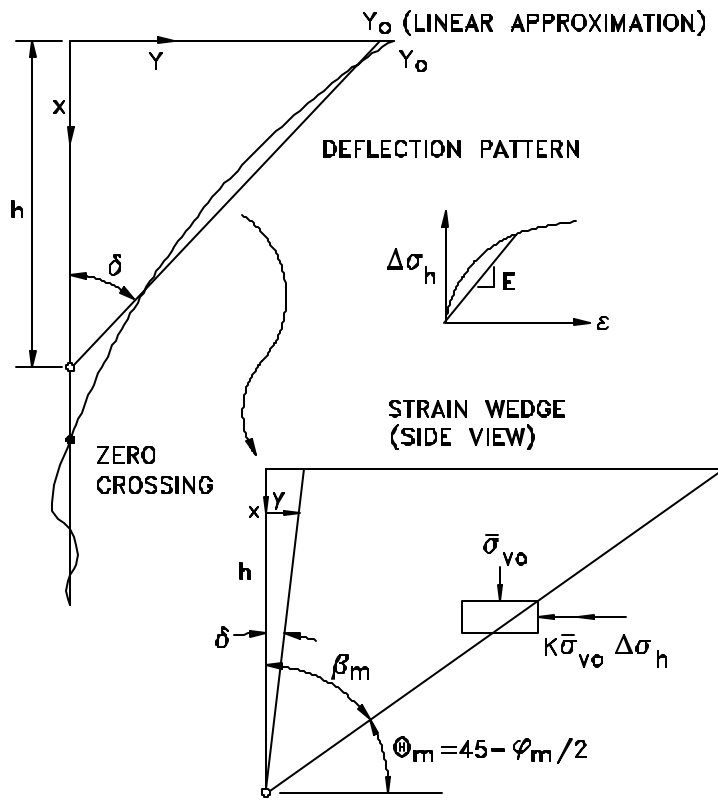
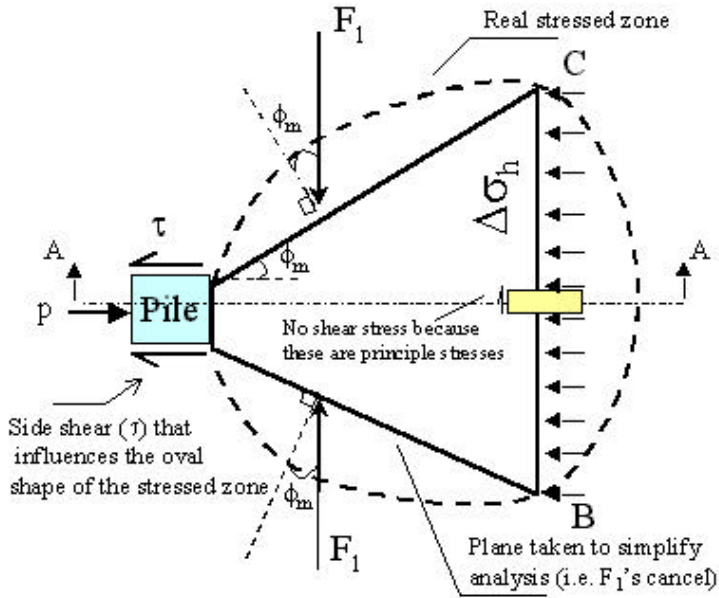
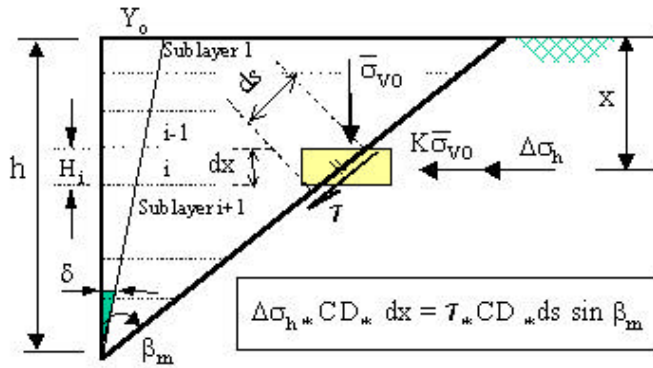


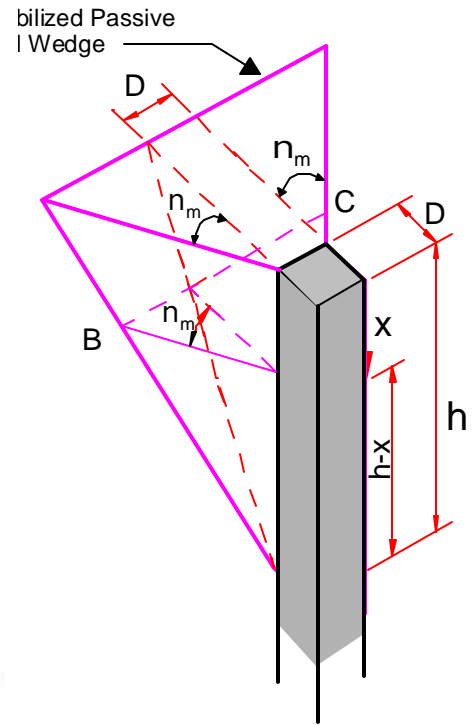
Fig. 5-3 Deflection Pattern of a Laterally Loaded Long Shaft/Pile and the Associated Strain Wedge



(b) Force equilibrium in a slice of the wedge at depth x



(c) Forces at the face of the soil passive wedge (Section elevation A-A)



(a) Basic Strain Wedge (SW) Model

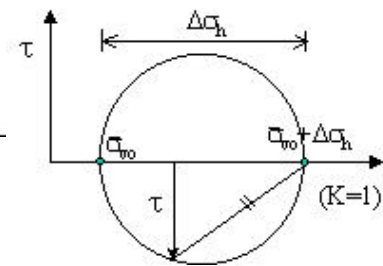


Fig. 5-4 Characterization and equilibrium of the SW model

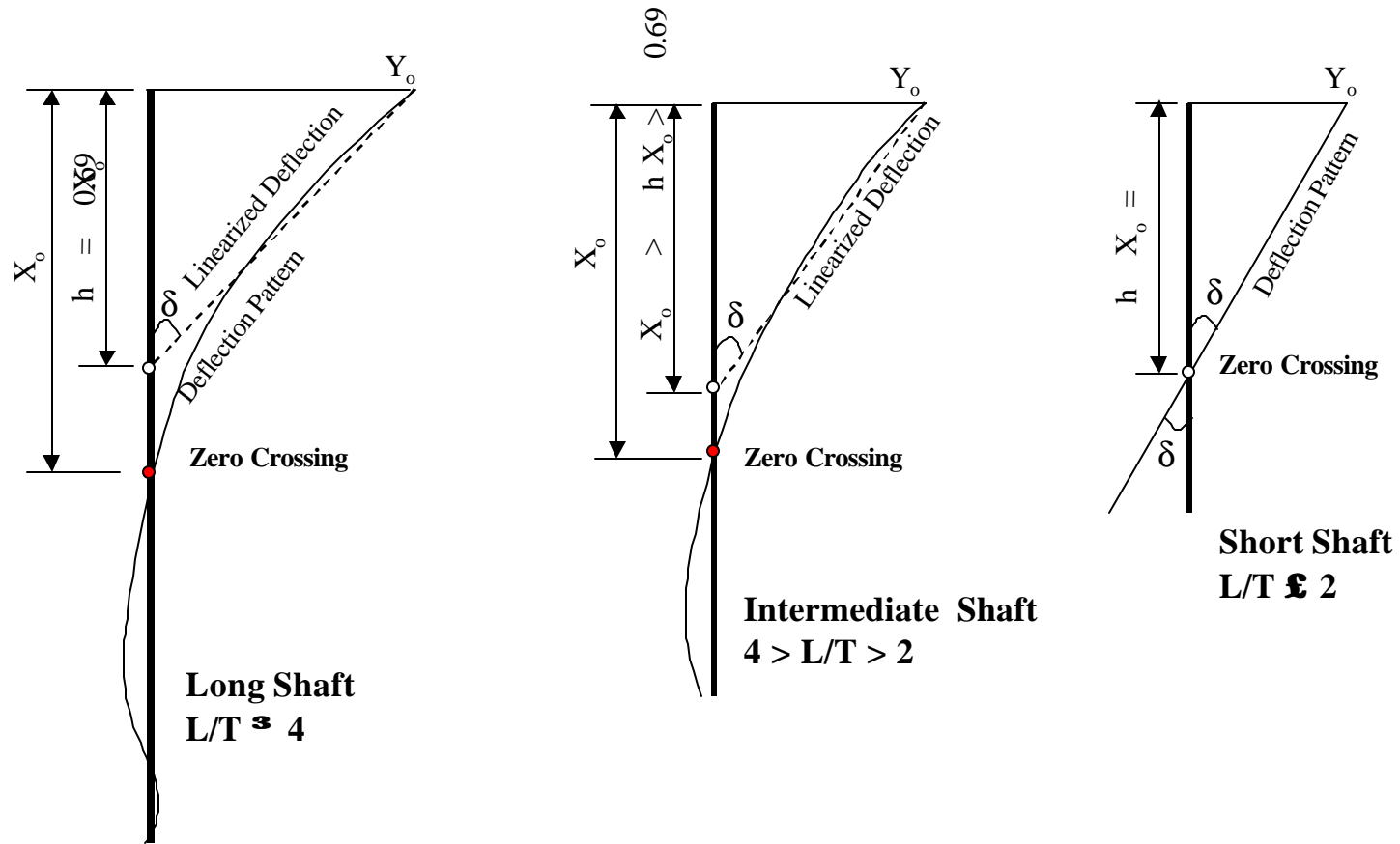


Fig. 5-5 Deflection Patterns of Long, Intermediate and Short Shafts

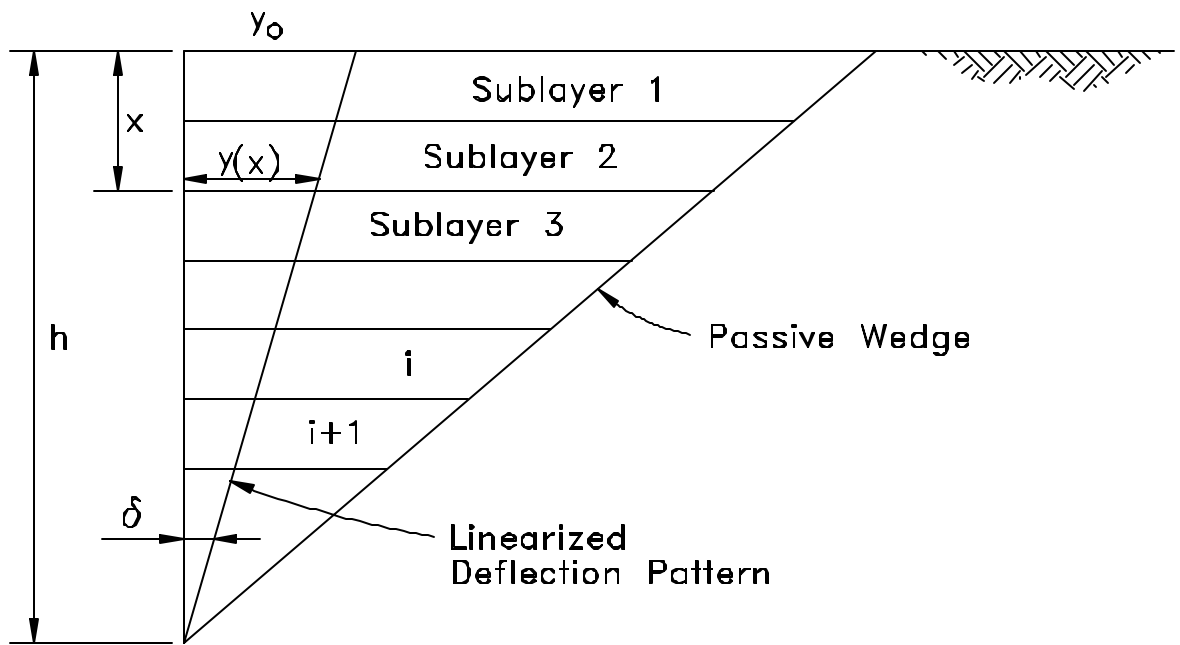


Fig. 5-7 The Linearized Deflection Pattern of a Pile/shaft Embedded in Soil Using the Multi Sublayer Strain Wedge Model

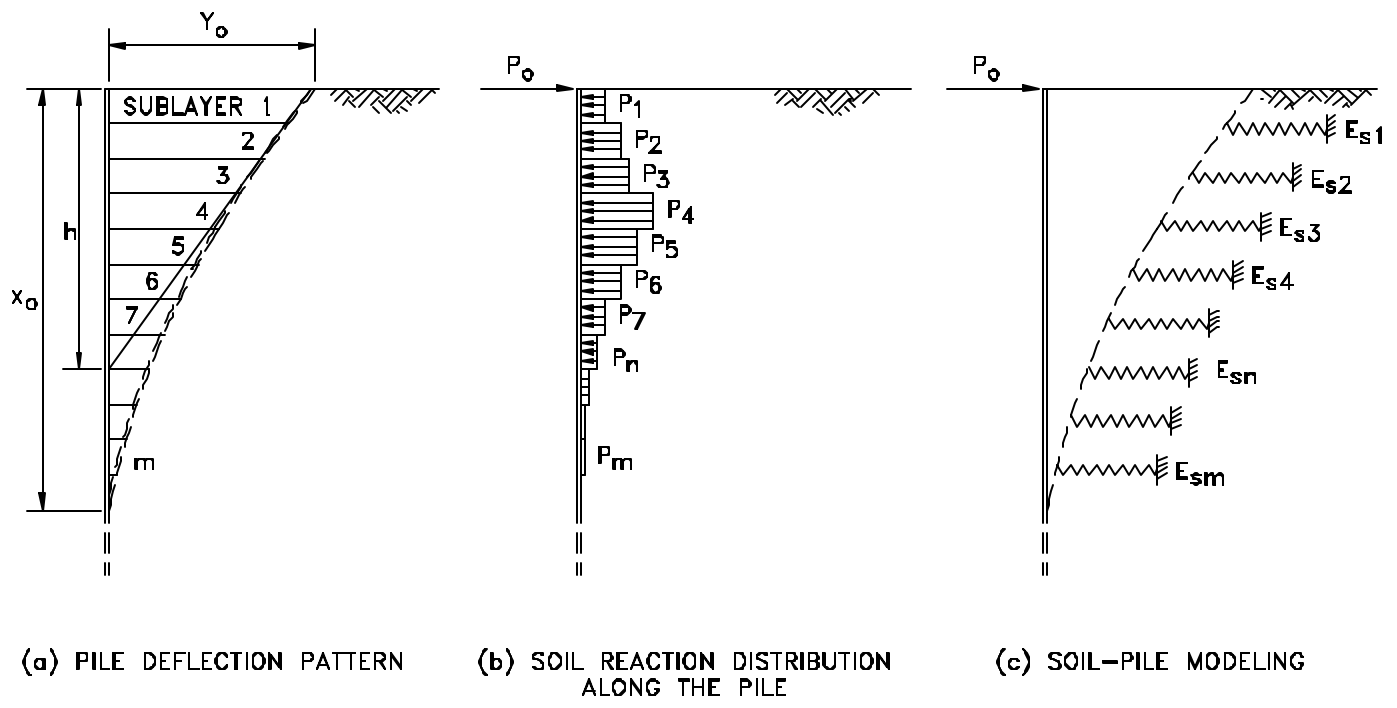


Fig. 5-8 Soil-Pile Interaction in the Multi-Sublayer Technique

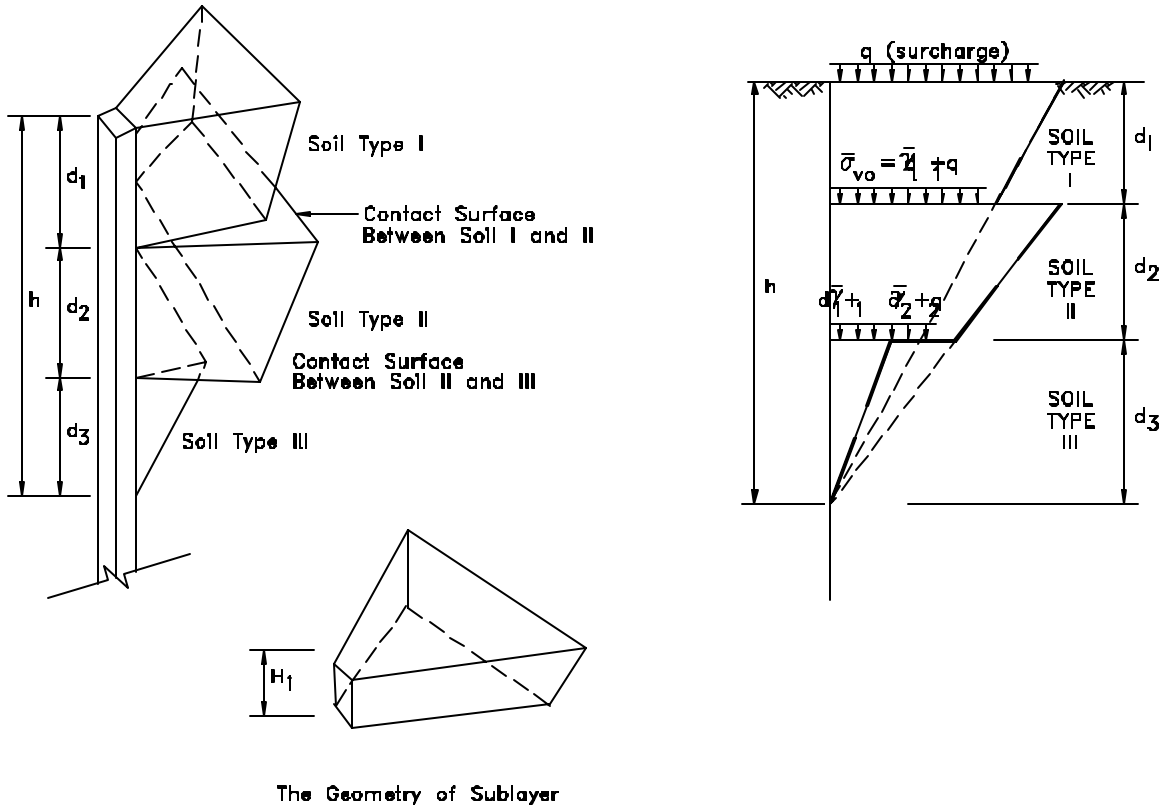


Fig. 5-9 The Proposed Geometry of the Compound Passive Wedge

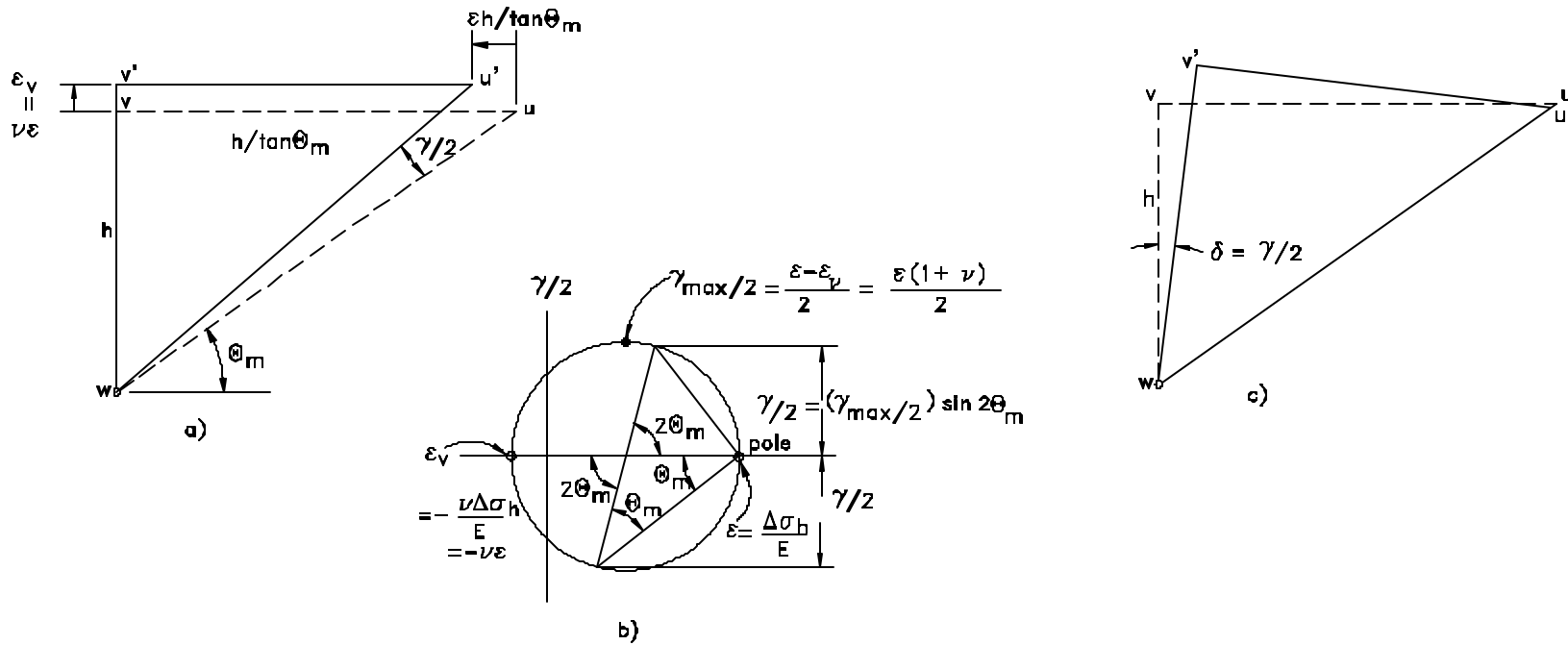


Fig. 5-10 Distortion of the Wedge a), The Associated Mohr Circle of Strain b), and the Relationship Between Pile Deflection and Wedge Distortion c)

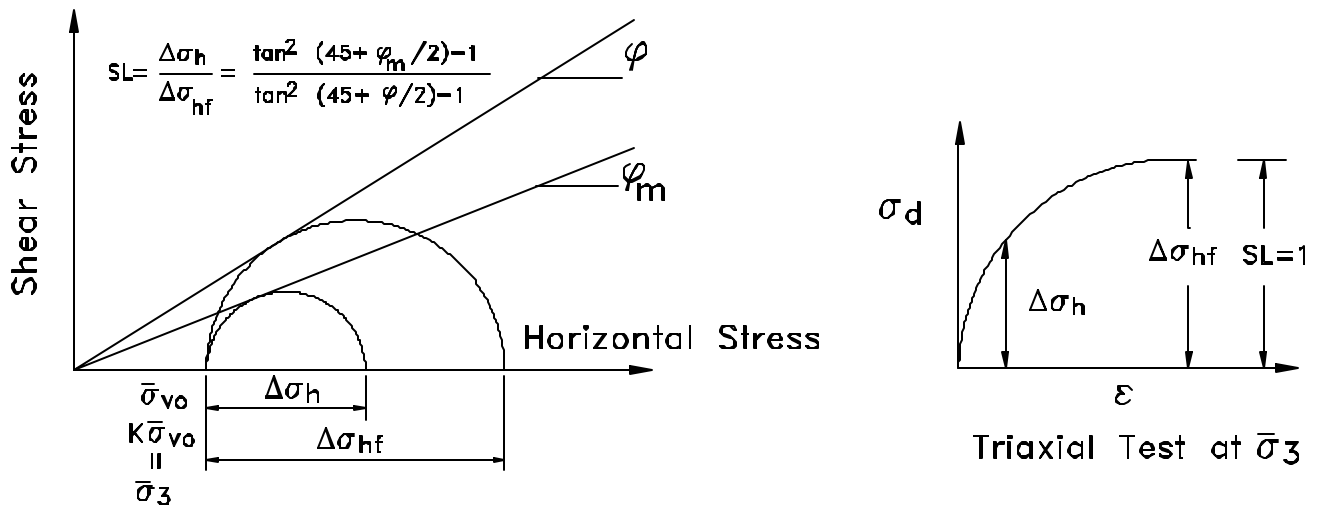
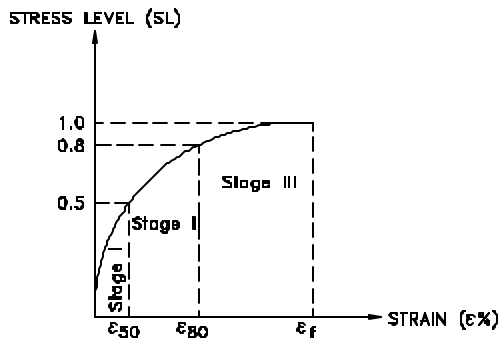
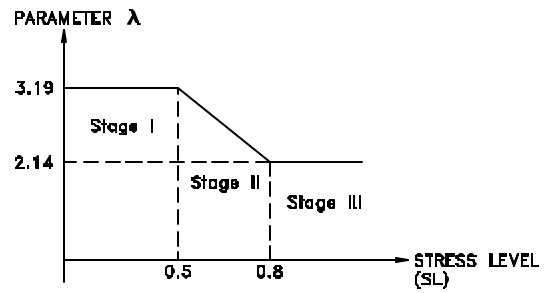


Fig. 5-11 Relationship Between Horizontal Stress Change, Stress Level, and Mobilized Friction Angle



(a) THE DEVELOPED HYPERBOLIC STRESS-STRAIN RELATIONSHIP IN SOIL



(b) THE VARIATION OF THE FITTING PARAMETER λ VERSUS STRESS LEVEL (SL)

Fig. 5-12 The Developed Stress-Strain Relationship in Soil

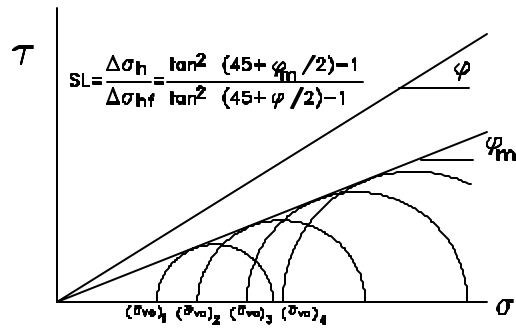
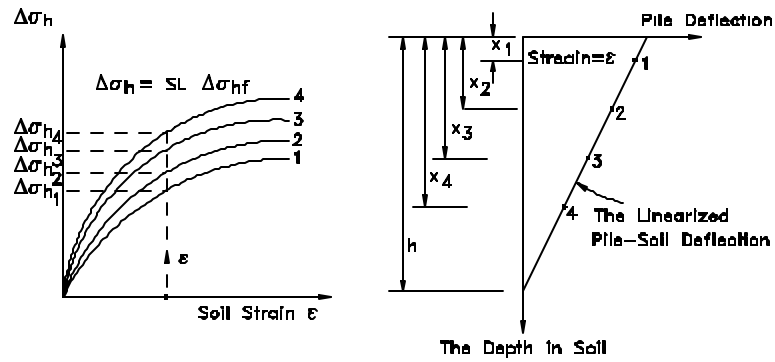


Fig. 5-13 The Nonlinear Variation of Stress Level Along the Depth of Soil at Constant Strain

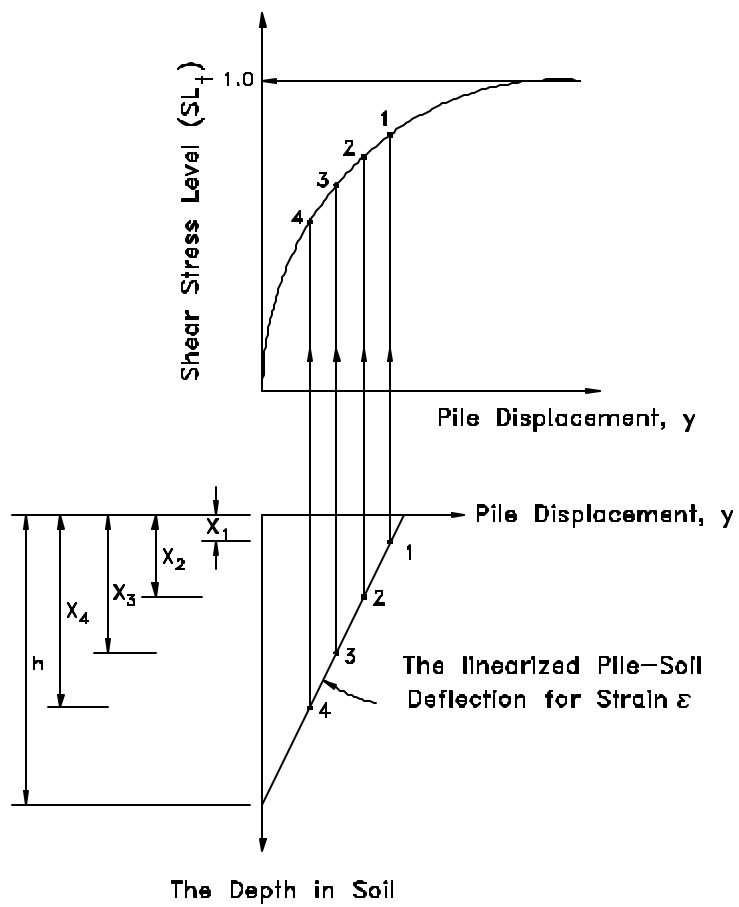
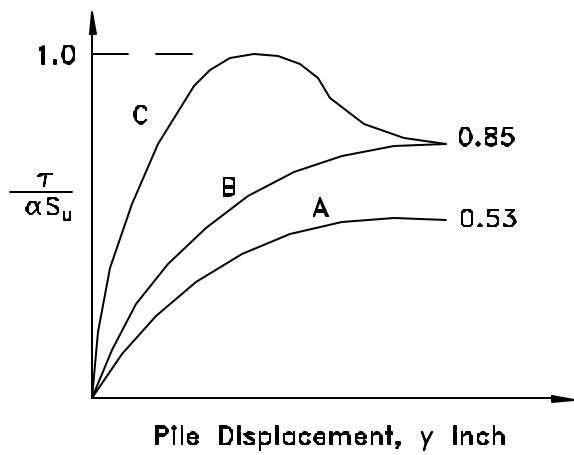
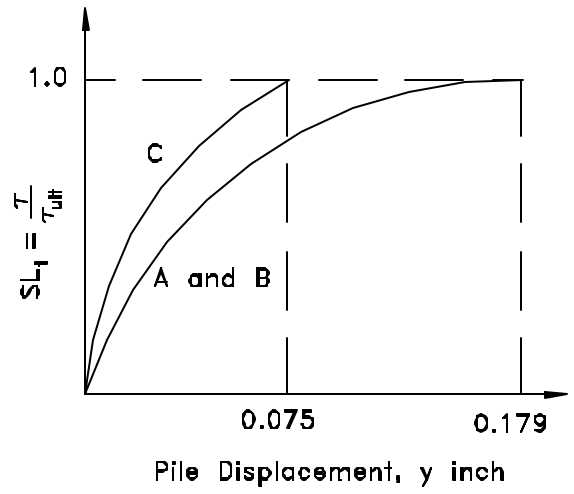


Fig. 5-14 The Employed Side Shear Stress-Displacement Curve in Clay



(a) Coyle-Reese Shear Stress Transfer Curve (t-z Curve)



(b) The Normalized t-z Curves

Fig. 5-15. The Nonlinear Variation of Shear Stress Level (SL_t) with depth in Clay

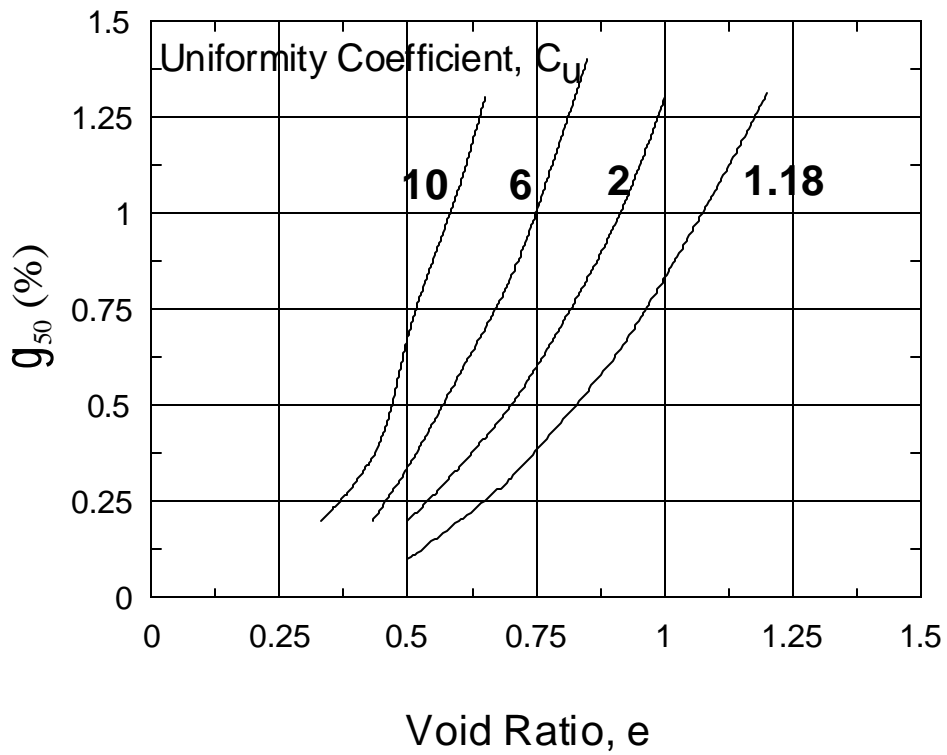


Fig. 5-16 Relationship Between e_{50} , Uniformity Coefficient (C_u) and Void Ratio (e) (Norris 1986)

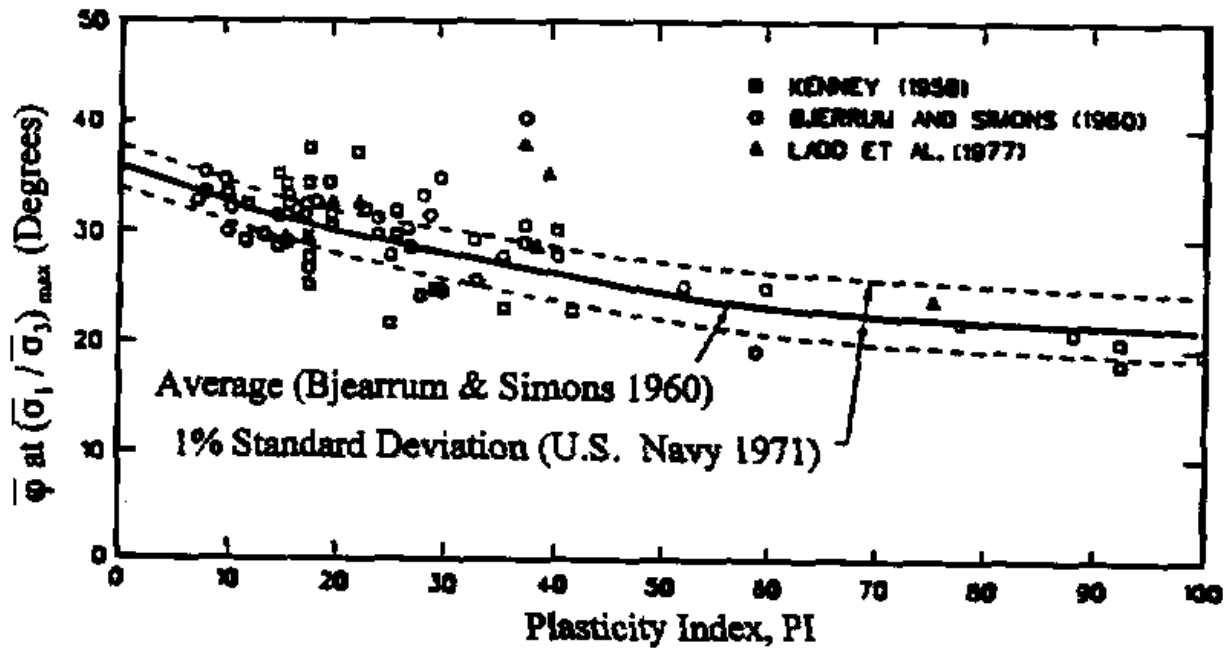
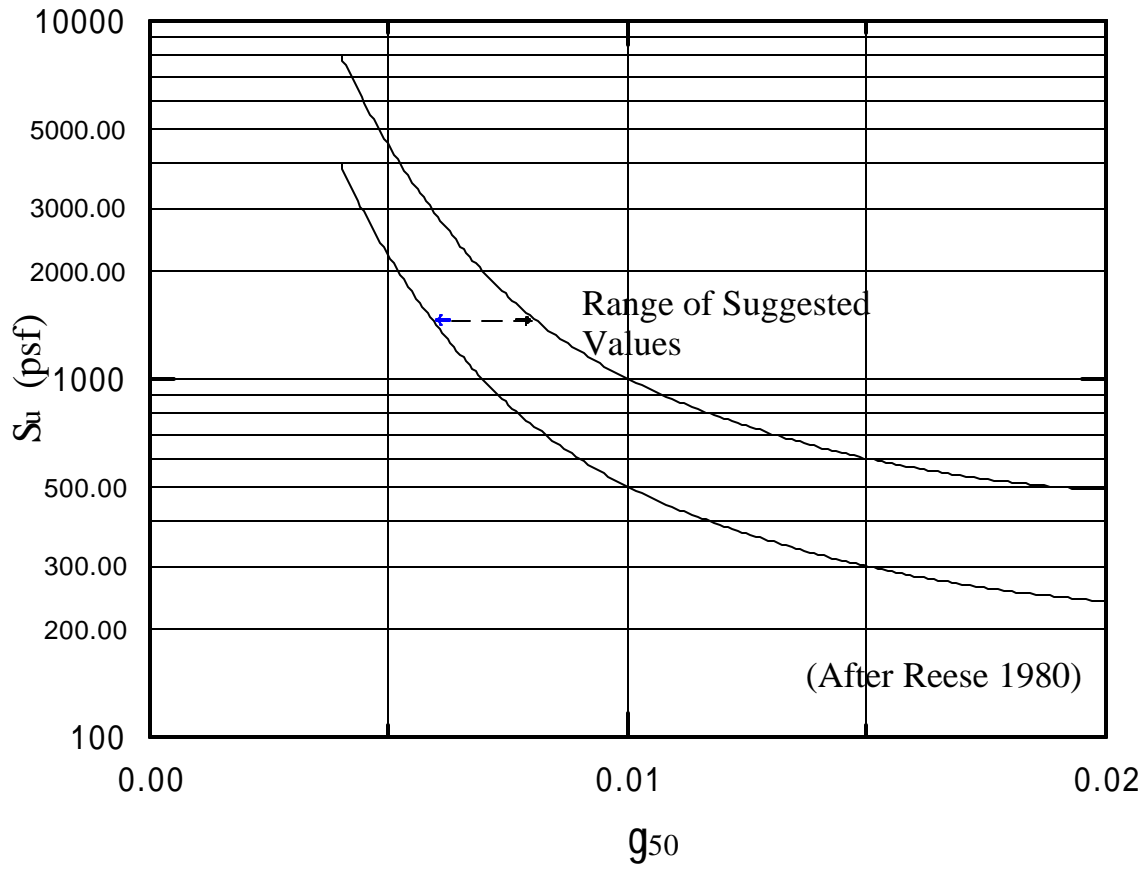


Fig. 5-17 Relationship Between Plasticity Index (PI) and Effective Stress Friction Angle (\bar{j}) (US Army Corps of Engineers 1996)



**Fig. 5-18 Relationship Between g_{50} and Undrained Shear Strength, S_u
(Evans and Duncan 1982)**

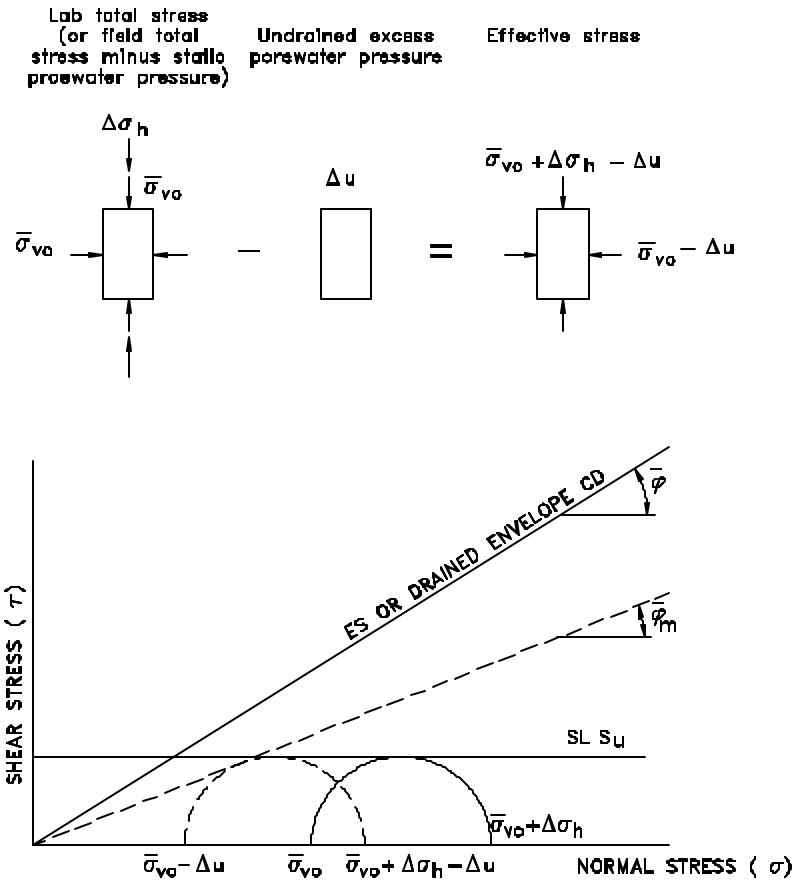


Fig. 5-19 Relationship Between Effective Stress and Total Stress Conditions

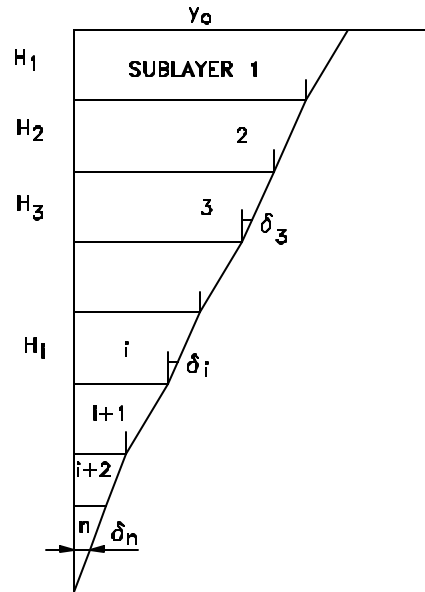


Fig. 5-20 The Assembling of Pile Head Deflection Using the Multi-Sublayer Technique

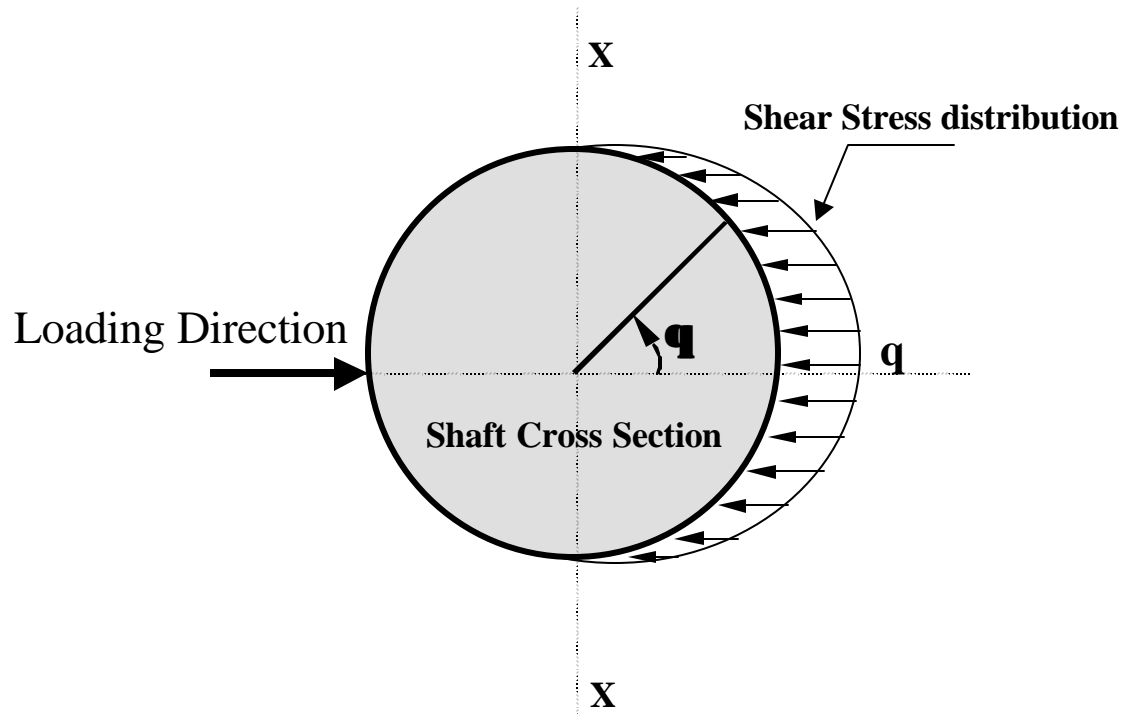


Fig. 5-21 Vertical Side Shear Stress Distribution on the Shaft Cross Section

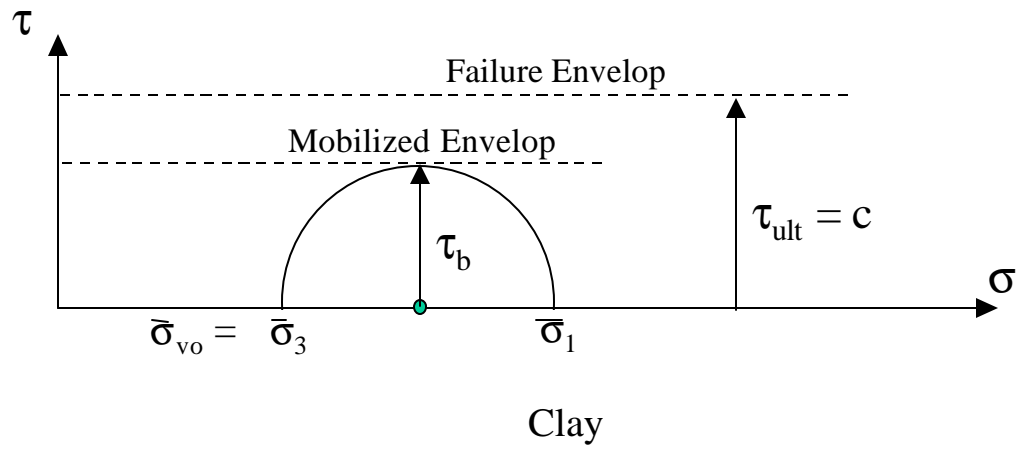
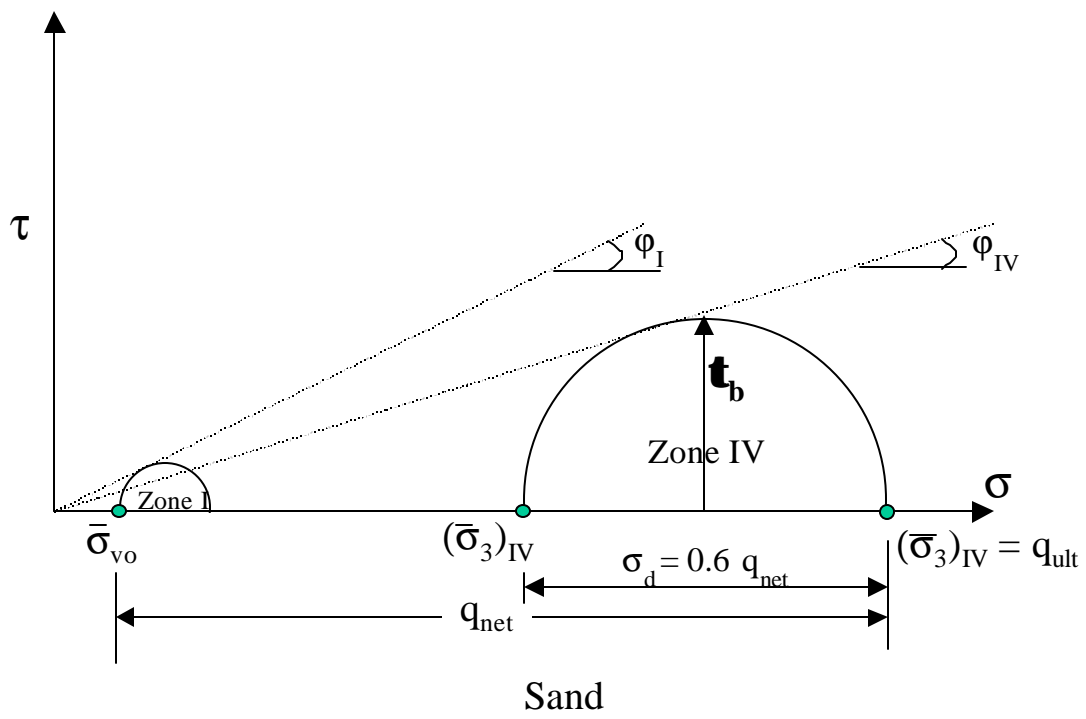


Fig. 5-22 Mobilized Shear Resistance at the Shaft Base in Sand and Clay